NANOSYSTEMS:
PHYSICS, CHEMISTRY, MATHEMATICS

Original article

Das M. *Nanosystems:*
Phys. Chem. Math., 2024, **15** (4), 473–480.
http://nanojournal.ifmo.ru
DOI 10.17586/2220-8054-2024-15-4-473-480

Diameter dependent geometrical and electrical properties of zigzag HgSe nanotubes: A density functional study

Monoj Das

Department of Physics, Gushkara Mahavidyalaya, Gushkara, 713128, India

dsmonoj@gmail.com

PACS 61.46.Fg, 71.20.-b, 73.63.Fg

ABSTRACT Using density functional theory, evolution of geometrical and electrical properties like wall width, binding energy, strain energy, band structure, density of states etc. of several zigzag HgSe nanotubes with diameters in the range of 11.59 to 21.74 Å are systematically investigated. It is noted that the walls of the nanotubes are gradually becoming thin with increasing tube diameter. This study reveals that the stability of the zigzag HgSe nanotube increases with increasing diameter. It is also perceived that zigzag HgSe nanotubes obey classical elasticity law. Band structure analysis reflects that all the zigzag HgSe nanotubes are direct band gap semiconductors and their band gaps slowly decrease with increasing diameter.

KEYWORDS nanotube, density functional theory, binding energy, band-gap

FOR CITATION Das M. Diameter dependent geometrical and electrical properties of zigzag HgSe nanotubes: A density functional study. *Nanosystems: Phys. Chem. Math.*, 2024, **15** (4), 473–480.

1. Introduction

The focal point of modern nanotechnology research is nanotubes owing to their vast potentials. Nanotubes may be successfully applied to a wide range of applications, such as field effect transistor, photovoltaic device, thermoelectric device, lasers, light emitting diodes and so on. For productive use of nanotubes in nanodevices, we must have a detail understanding of their characteristics. Synthesis of carbon nanotube [1] expedited the research on nanotubes and consequently nanotubes of many non-carbon materials like BN, SiC, CdS, ZnO, ZnS, WS_2, MoS_2, CdSe [2–8] etc. were synthesized. Recently, HgSe based nanostructures are seeking enormous attention attributed to their lucrative properties such as high electron mobility, high electron density, etc. [9]. In bulk form, HgSe has nearly zero band gap making it a semimetal [10]. Various types of nanostructures such as nanorods, nanowires, nano particles, quantum dots, thin film etc. of this material have already been synthesized [11–18]. In addition, HgSe nanotubes are also synthesized. R. R. Arnepalli et al. [19] first synthesized HgSe nanotubes by spray deposition of solvothermally synthesized HgSe-Iodine nanoparticles. R. R. Arnepalli et al. [20] also synthesized multi walled HgSe nanotubes by employing mercury iodide catalyst. Various forms of HgSe nanostructures are successfully utilized in mid infrared photo detector, thermoelectric devices, leds etc. [21–28]. For many years, HgSe has been the subject of many theoretical studies. By employing linear muffin-tin orbital method Delin et al. [29] reported that HgSe in zinc-blende phase exhibits semi-metallic property. Radescu et al. [30] studied the pressure-driven phase transitions in HgSe. Employing density functional theory, Duz et al. [31] investigated the mechanical properties of HgSe polymorphs under high pressure. The structural, electrical, optical and thermodynamic features of HgSe crystal are reported by Secuk et al. [32]. Using density functional theory, Li et al. [33] reported that under in plane tensile strain, HgSe monolayer endured insulator to topological insulator phase transition. Very recently, Habibes et al. [34] studied the electronic and optical properties of Mn doped HgSe for spintronic device applications. However, as of yet, no theoretical work on HgSe nanotubes has been published. To use HgSe nanotubes in a range of nanodevices, it is essential to understand their properties. Here, for the first time, the properties of zigzag HgSe nanotubes are reported using density functional theory. At this point, it is important to highlight that density functional theory underestimates the band gap value in semiconductors. However, we can get a qualitative view of the trend of band gap variation of a nanotube with respect to diameter. Moreover, several researchers have used density functional theory to study the properties of HgSe nanostructures and some findings (such as semi metallic property) agree with the experimental observations. Therefore, density functional theory can be used to predict the properties of zigzag HgSe nanotubes. In the following section, the methods and important parameters are described. The results are enumerated in Section 3 and finally the significant findings are summarized in Section 4.

2. Approach and method

The geometrical and electronic properties of zigzag HgSe nanotubes are extracted by using SIESTA package [35, 36] that implements Density Functional Theory. The exchange and correlation energy is represented by generalized gradient approximated (GGA) Perdew–Burke–Ernzerhof (PBE) functional [37]. The Monkhorst–Pack method [38] with

a 25×1×1 K-point mesh is used to sample the Brillouin Zone. Throughout the calculations, the real space mesh cut-off energy is taken as 460 Ry. The energy convergence limit for self-consistent fields (SCF) is set at 10^{-5} eV. During all the calculations, a vacuum space of 25 Å is kept so as to neglect interaction between the nanotube and its periodic image. The most favourable geometry is obtained by setting force convergence limit to 0.001 eV/Å.

In this study, HgSe nanosheet (HgSeNS) as depicted in Fig. 1 is rolled along the chiral vector $\vec{\mathbf{C}} = x\vec{\mathbf{u}} + y\vec{\mathbf{v}}$ to obtain HgSe(x, y) nanotube. The tube axis is always perpendicular to the chiral vector. For zigzag nanotubes, $y = 0$. Here, the properties of HgSe(8,0) to HgSe(15,0) are investigated systematically.

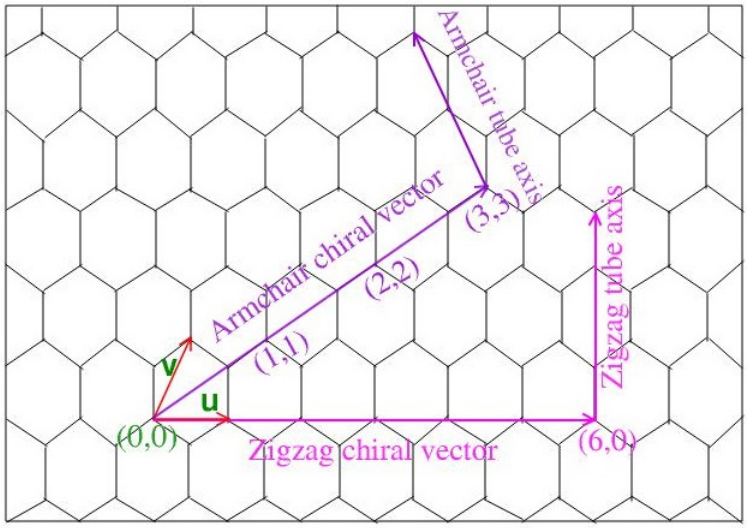

FIG. 1. The chiral vector and tube axis in HgSe nanosheet

3. Results and discussions

Initially, the HgSe nanosheet's relaxed geometrical structure is identified. It is perceived that the relaxed HgSeNS is buckled like having a buckled height of 0.39 Å. The mean Hg–Se bond length in HgSeNS is 2.62 Å. The optimized structure of HgSeNS is displayed in Fig. 2.

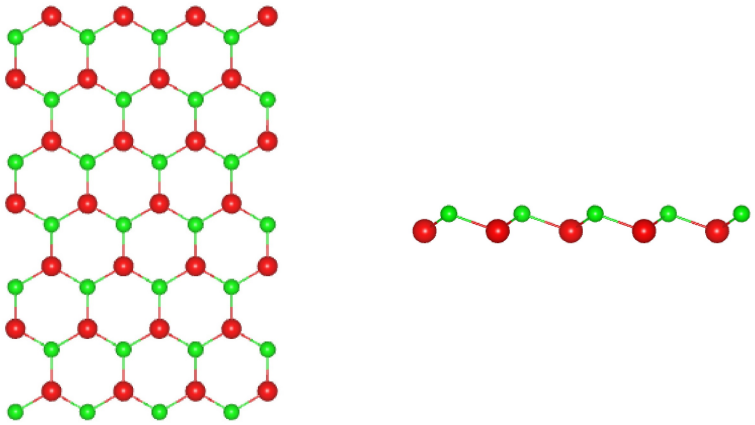

(a) Top view (b) Side view

FIG. 2. Optimized geometrical structure of HgSe nanosheet. The bigger (red) spheres represent Hg atoms and smaller (green) spheres denote Se atoms respectively

This optimized nanosheet is adopted to construct various zigzag HgSe nanotubes (ZHgSeNTs) by folding this sheet along various zigzag chiral vectors. These nanotubes are allowed to undergo further relaxation. After relaxation, the nanotube surfaces take wave like pattern as depicted in Fig. 3. The more electronegative Se atoms move away from the axis compared to the Hg atoms. Thus, it appears that the surface of the nanotube is composed of two coaxial cylinders, with Se atoms arranged on the outer cylinder and Hg atoms on the inner cylinder. Note that, the strong covalent bonds continue

to hold the Hg atoms in the inner cylinder and the Se atoms in the outer cylinder together. Similar surface configurations have also been observed in nanotubes made of AlN, CdS, ZnTe [39–41] etc. The wall width of the nanotubes can be calculated by measuring the difference in radius between the inner and outer cylinders. Wall widths of all the nanotubes are estimated and are displayed in the Table 1. The variation of wall width with respect to diameter is also presented in Fig. 4. Calculations show that the wall width of zigzag HgSe nanotube steadily decreases from 0.547 to 0.421 Å upon increasing diameter from 11.59 to 21.74 Å. Therefore, nanotube walls are progressively becoming thin with enlarging tube diameter. It is important to mention that wall thickness is an indicator of surface buckling in nanotubes. When a nanosheet is rolled into a nanotube, strain or deformation related to this process causes buckling in the nanotube surface. In comparison to larger diameter nanotubes, those with a smaller diameter exhibit more buckling and, thus, a thicker wall due to their higher strain energy.

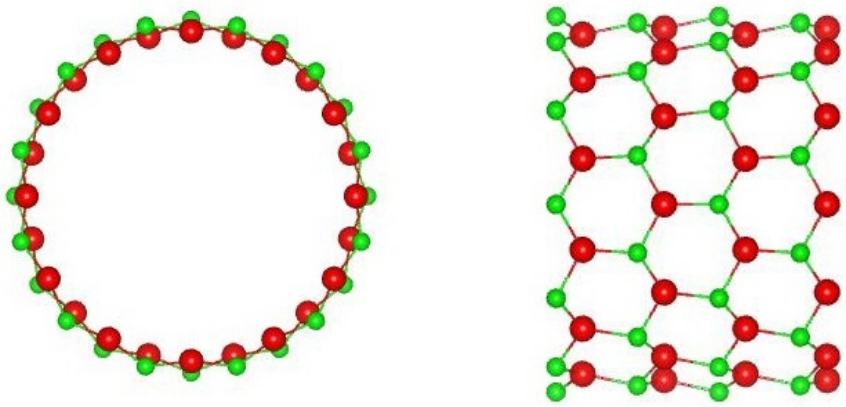

(a) Top view (b) Side view

FIG. 3. Energetically relaxed geometrical structure of HgSe(12,0) nanotube. The bigger (red) spheres indicate Hg atoms and smaller (green) balls represent Se atoms respectively

TABLE 1. Diameter, wall thickness, binding energy, strain energy, band gap values of various zigzag HgSe nanotubes

Nanotube	Diameter (Å)	Wall Thickness (Å)	Binding Energy (eV)	Strain Energy (eV)	Band Gap (eV)
HgSe(8,0)	11.59	0.547	1.918	0.071	0.60
HgSe(9,0)	13.08	0.523	1.927	0.062	0.55
HgSe(10,0)	14.50	0.502	1.934	0.055	0.51
HgSe(11,0)	15.96	0.483	1.940	0.049	0.47
HgSe(12,0)	17.40	0.466	1.944	0.045	0.43
HgSe(13,0)	18.85	0.450	1.948	0.041	0.39
HgSe(14,0)	20.30	0.435	1.951	0.038	0.35
HgSe(15,0)	21.74	0.421	1.954	0.035	0.32

The stability of HgSe nanosheet and various zigzag HgSe nanotubes can be assessed by determining their binding energies using the following formula:

$$E_{BE} = -\frac{E\,(\mathrm{HgSe}) - NE\,(\mathrm{Hg}) - NE(\mathrm{Se})}{2N}.$$

Here, $E(\mathrm{HgSe})$ represents the total energy of relaxed HgSe nanosheet or nanotube consisting of N Hg and N Se atoms. $E(\mathrm{Hg})$ and $E(\mathrm{Se})$ denote energy of isolated Hg and Se atom, respectively. It is observed that the binding energy of

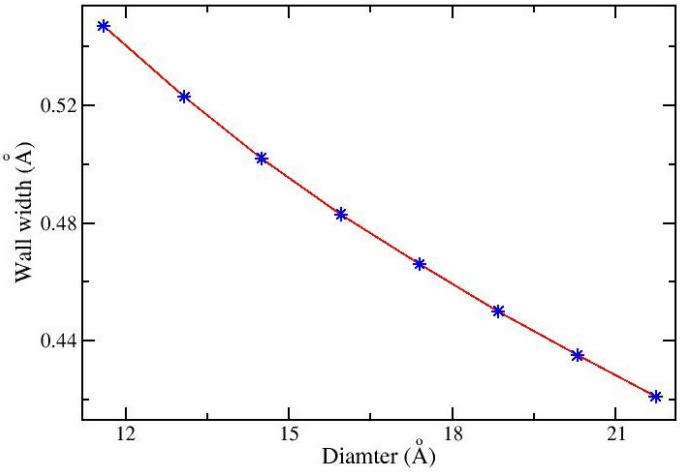

FIG. 4. Plot of wall thickness vs. diameter of zigzag HgSe nanotubes

HgSeNS is 1.989 eV. The binding energies of ZHgSeNTs are determined and written in Table 1. The variation of binding energy with respect to diameter is also graphically plotted in Fig. 5. The binding energy of ZHgSeNT is increasing from 1.918 to 1.954 eV when the diameter is altered from 11.59 to 21.74 Å. Therefore, ZHgSeNTs with smaller diameters are relatively less stable than those with greater diameters. This can be explained by the fact that decreasing the diameter causes the bond to bend more, reducing the stability.

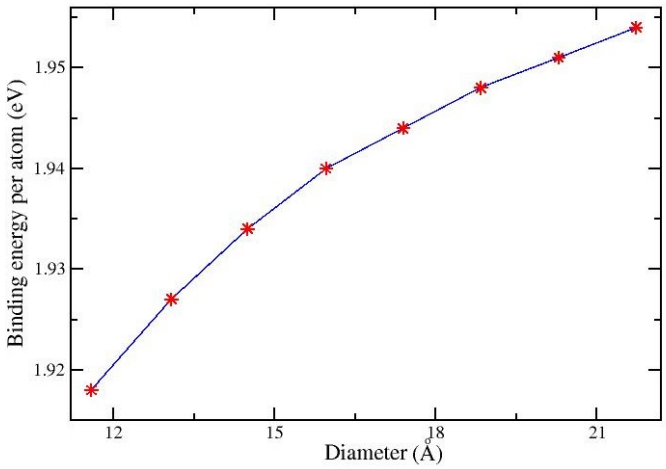

FIG. 5. Variation of binding energy per atom as a function of tube diameter of zigzag HgSe nanotubes

To figure out the energy required to create HgSe nanotubes with different diameters from HgSe nanosheet, the strain energies of HgSe nanotubes are evaluated. The strain energy, E_s is just the binding energy difference between HgSeNS and ZHgSeNT, i.e.

$$E_s = E_{BE}\,(\text{HgSeNS}) - E_{BE}\,(\text{ZHgSeNT})\,.$$

Here, E_{BE}(HgSeNS) and E_{BE}(ZHgSeNT) represent binding energy of HgSe nanosheet and zigzag HgSe nanotube, respectively. The estimated strain energy of every nanotube is displayed in Table 1. The classical continuum elasticity theory reflects that strain energy, E_s, must vary as $E_s = m/D^2 + c$ against diameter (D) where m and c are constants [42]. The strain energy is plotted against $1/D^2$ in Fig. 6 to determine whether ZHgSeNTs comply with classical elasticity theory or not. The straight line nature of the plot signifies that ZHgSeNTs obey classical elasticity theory. The values of the constants m and c, according to least square fitting, are 6.744 and 0.022, respectively.

One of the important electrical characteristics of a material is its band gap, which dictates the material's use in technological applications. In nanoelectronics, figuring out different ways to accomplish band gap engineering is also crucial. The band gaps of HgSeNS and ZHgSeNTs are estimated in order to evaluate the importance of these nanostructures in different technological applications. The findings are shown in Table 1. The variation of band gap in terms of nanotube diameter is also plotted in Fig. 7. It is marked that HgSeNS is a low direct band gap semiconductor with a band gap of 0.12 eV as shown in Fig. 8. Band structures of various ZHgSeNTs are also depicted in Fig. 9. It is perceived that all

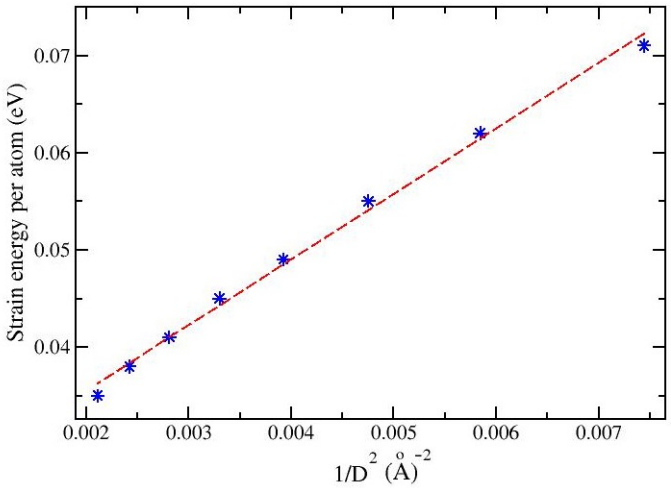

FIG. 6. The plot of strain energy per atom as a function of $1/D^2$. The best fit curve is shown by the dotted line

the ZHgSeNTs are direct band gap semiconductors and their band gaps are slowly decreasing from 0.60 to 0.32 eV when diameter is increased from 11.59 to 21.74 Å. Therefore, one can tune band gap within a range of 0.28 eV by altering diameter from 11.59 to 21.74 Å. This trend of decreasing band gap with increasing tube diameter is in the same line with other II–VI semiconductors like CdS, ZnTe, ZnO, ZnS etc. nanotubes [40, 41, 43, 44]. It is commonly recognised that II–VI semiconductors show the quantum confinement effect, in which the band gap widens as the nanostructure's size decreases. This quantum confinement effect can account for the band gap rise in zigzag HgSe nanotubes with decreasing nanotube diameter.

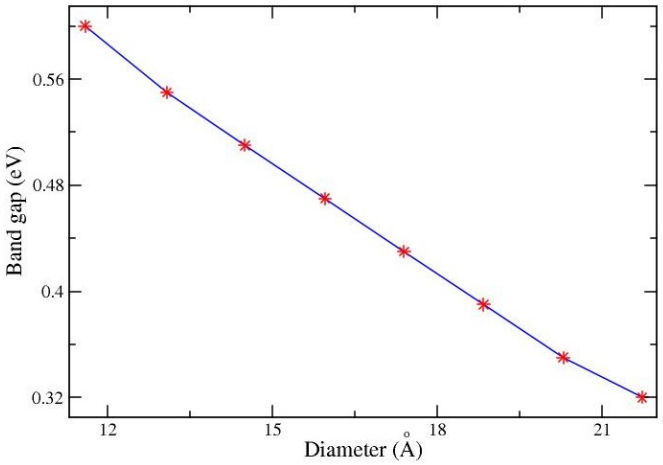

FIG. 7. Band gap vs. diameter plot of zigzag HgSe nanotubes

To support the pattern of decreasing band gap with increasing tube diameter, the total density of states of various ZHgSeNTs are determined and displayed in Fig. 10. This graph makes it very evident that the band gap becomes smaller for nanotube of larger diameter.

4. Summary

In conclusion, density functional theory is used to present the variation of geometrical and electrical properties with respect to diameter of various zigzag HgSe nanotubes. It is predicted that the walls of the nanotubes gradually get thinner as the diameters of the nanotubes increase. It is further noticed that zigzag HgSe nanotubes become increasingly stable on increasing their diameter. Strain energy analysis manifests that all the zigzag HgSe nanotubes adhere to the classical elasticity law. Band structure calculation signifies that the variation of band gap with diameter is congruous with other II–VI semiconductor nanotubes and the band gap energy may be calibrated over practically useful range of 0.32 to 0.60 eV. These results might help to expedite future studies on HgSe nanotubes.

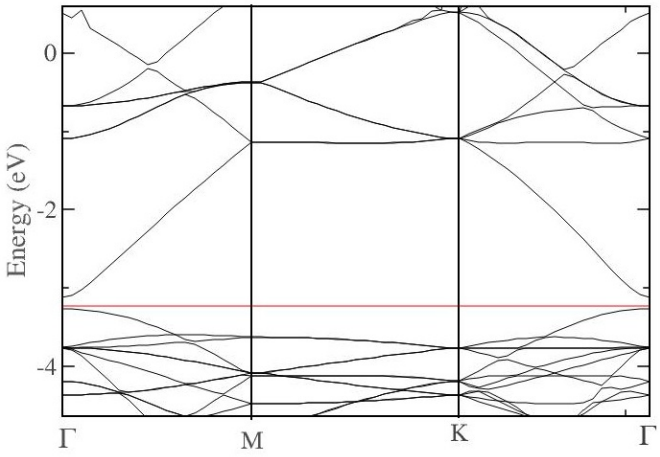

FIG. 8. Band structure plot of HgSe nanosheet. The fermi energy level is shown by the solid red line

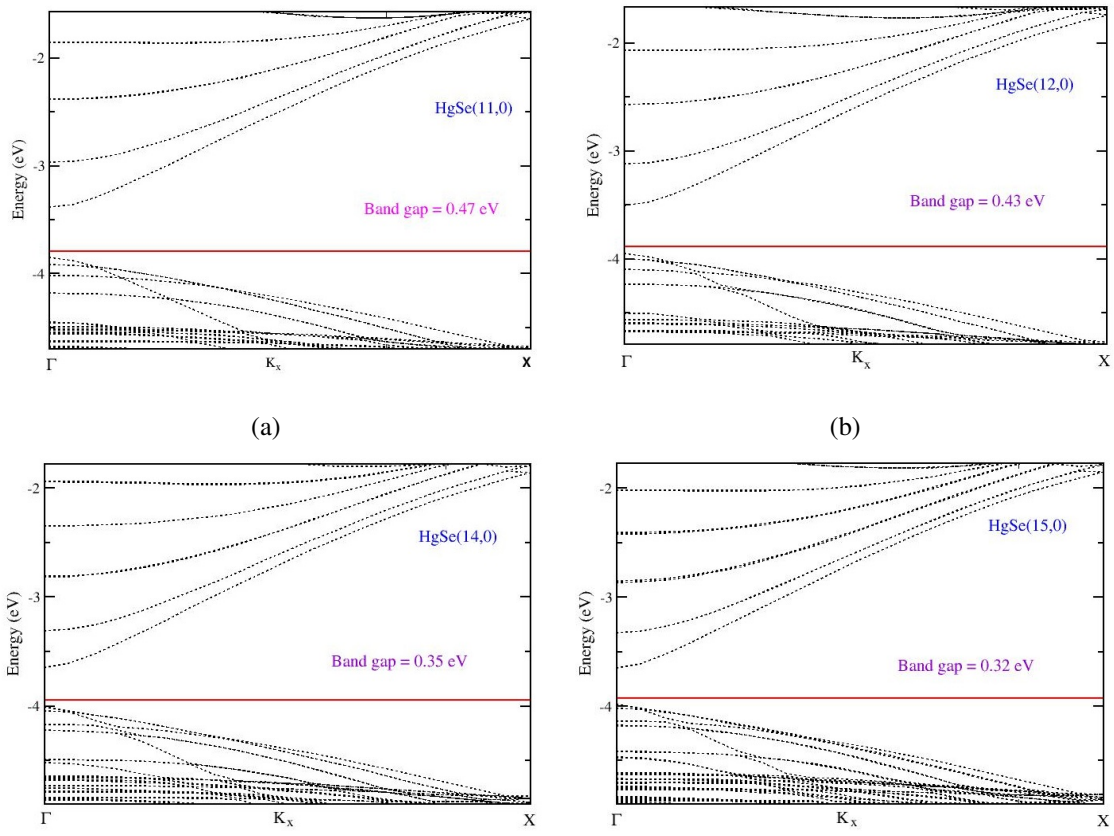

FIG. 9. Band structure plots of various zigzag HgSe nanotubes. The fermi energy level is represented by the solid red line

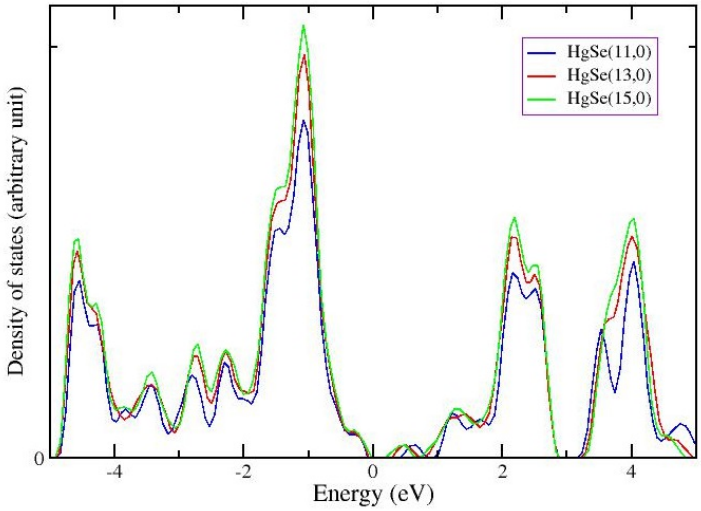

FIG. 10. The total density of states plot of different zigzag HgSe nanotubes. Here, the Fermi energy is scaled down to zero

References

[1] Iijima S. Helical microtubules of graphitic carbon. *Nature*, 1991, **354**, P. 56–58.

[2] Chopra N.G. et al. Boron Nitride Nanotubes. *Science*, 1995, **269** (5226), P. 966–967.

[3] Huu C.P., Keller N., Ehret G., Ledoux M.J. The First Preparation of Silicon Carbide Nanotubes by Shape Memory Synthesis and Their Catalytic Potential. *J. of Catalysis*, 2001, **200** (2), P. 400–410.

[4] Ling T., Wu M., Du X. Template synthesis and photovoltaic application of CdS nanotube arrays. *Semiconductor Science and Technology*, 2012, **27** (5), 055017.

[5] Madlol R.A.A. Structural and optical properties of ZnO nanotube synthesis via novel method. *Results in Physics*, 2017, **7**, P. 1498–1503.

[6] Guo M., Song M., Li S., Yin Z., Song X., Bu Y. Facile and economical synthesis of ZnS nanotubes and their superior adsorption performance for organic dyes. *Cryst. Eng. Comm.*, 2017, **19**, P. 2380–2393.

[7] Sinha S.S., Yadgarov L., Aliev S.B., Feldman Y., Pinkas I., Chithaiah P., Ghosh S., Idelevich A., Zak A., Tenne R. MoS_2 and WS_2 Nanotubes: Synthesis, Structural Elucidation, and Optical Characterization. *The J. of Physical Chemistry C*, 2021, **125** (11), P. 6324–6340.

[8] Shen Q., Jiang L., Miao J., Hou W., Zhu J.J. Sonoelectrochemical synthesis of CdSe nanotubes. *Chem. Commun.*, 2008, **14**, P. 1683–1685.

[9] Ren J., Eason D.B., Churchill L.E., Yu Z., Boney C., et al. Integrated heterostructure devices composed of II–VI materials with Hg-based contact layers. *J. of Crystal Growth*, 1994, **138**, P. 455–463.

[10] Truchseß M.V., Pfeuffer-Jeschke A., Becker C.R., Landwehr G., Batke E. Electronic band structure of HgSe from Fourier transform spectroscopy. *Phys. Rev. B*, 2000, **61**, 1666.

[11] Ding T., Zhang J.R., Hong J.M., Zhu J.J., Chen H.Y. Sonochemical synthesis of taper shaped HgSe nanorods in polyol solvent. *J. of Crystal Growth*, 2004, **260**, P. 527–531.

[12] Zare M.E., Niasari M.S., Sobhani A. Simple sonochemical synthesis and characterization of HgSe nanoparticles. *Ultrasonics Sonochemistry*, 2012, **19** (5), P. 1079–1086.

[13] Ding T., Zhu J.J., Hong J.M. Sonochemical preparation of HgSe nanoparticles by using different reductants. *Materials Letters*, 2003, **57**, P. 4445–4449.

[14] Wang S., Guo T., Cao S. The Influence of Synthetic Parameters on HgSe QDs. *ACS Omega*, 2023, **8** (47), P. 44804–44811.

[15] Mahalingam T., Kathalingam A., Sanjeeviraja C., Chandramohan R., Chu J.P, Kim Y.D., Velumani S. Electrodeposition and characterization of HgSe thin films. *Materials Characterization*, 2007, **58** (8–9), P. 735–739.

[16] Hankare P.P., Bhuse V.M., Garadkar K.M., Jadhav A.D. A novel method to grow polycrystalline HgSe thin film. *Materials Chemistry and Physics*, 2001, **71** (1), P. 53–57.

[17] Hankare P.P., Bhuse V.M., Garadkar K.M., Delekar S.D., Mulla I.S. Chemical deposition of cubic CdSe and HgSe thin films and their characterization. *Semiconductor Science and Technology*, 2004, **19**, 70.

[18] Bazarganipour M., Sadri M., Davar F., Niasari M.S. Mercury selenide nanorods: Synthesis and characterization via a simple hydrothermal method. *Polyhedron*, 2011, **30** (6), P. 1103–1107.

[19] Arnepalli R.R., Dutta V. Nanotubes in Low Temperature Spray Deposited Nanocrystalline HgSe: I thin films. *MRS Online Proceedings Library*, 2006, **922**, 209.

[20] Arnepalli R.R., Dutta V., Singh V.N. Multiwalled HgX (X = S, Se, Te) Nanotubes Formed with a Mercury Iodide Catalyst in Nanocrystalline Thin Films Spray-Deposited at Low Temperature. *Advanced Materials*, 2008, **20** (10), P. 1945–1951.

[21] Jana M.K., Chithaiah P., Murali B., Krupanidhi S.B., Biswasa K., Rao C.N.R. Near infrared detectors based on HgSe and HgCdSe quantum dots generated at the liquid-liquid interface. *J. Mater. Chem. C*, 2013, **1**, P. 6184–6187.

[22] Chen M., Hao Q., Luo Y., Tang X. Mid-Infrared Intraband Photodetector via High Carrier Mobility HgSe Colloidal Quantum Dots. *ACS Nano*, 2022, **16** (7), P. 11027–11035.

[23] Zhao X., Mu G., Tang X., Chen M. Mid-IR Intraband Photodetectors with Colloidal Quantum Dots. *Coatings*, 2022, **12** (4), 467.

[24] Hao Q., Ma H., Xing X., Tang X., Wei Z., Zhao X., Chen M. Mercury Chalcogenide Colloidal Quantum Dots for Infrared Photodetectors. *Materials*, 2023, **16** (23), 7321.

[25] Prudnikau A., Roshan H., Paulus F., García B.M., Hübner R., Jalali H.B., Franco M.D., Prato M., Stasio F.D., Lesnyak V. Efficient Near-Infrared Light-Emitting Diodes Based on CdHgSe Nanoplatelets. *Advanced Functional Materials*, 2024, **34**, 2310067.

[26] Hodges J.M., Hao S., Grovogui J.A., Zhang X., Bailey T.P., Li X., Gan Z., Hu Y.Y., Uher C., Dravid V.P., Wolverton C., Kanatzidis M.G. Chemical Insights into PbSe – $x\%$ HgSe: High Power Factor and Improved Thermoelectric Performance by Alloying with Discordant Atoms. *J. of the American Chemical Society*, 2018, **140** (51), P. 18115–18123.
[27] Yun J., Cho K., Park Y., Yang S., Choi J., Kim S. Thermoelectric characteristics of nanocomposites made of HgSe and Ag nanoparticles for flexible thermoelectric devices. *Nano Research*, 2017, **10** (2), P. 683–689.
[28] Tang X., Wua G.F., Lai K.W.C. Plasmon resonance enhanced colloidal HgSe quantum dot filterless narrowband photodetectors for mid-wave infrared. *J. Mater. Chem. C*, 2017, **5**, P. 362–369.
[29] Delin A., Klüner T. Excitation spectra and ground-state properties from density-functional theory for the inverted band-structure systems β-HgS, HgSe, and HgTe. *Phys. Rev. B*, 2002, **66**, 035117.
[30] Radescu S., Mujica A., López-Solano J., Needs R.J. Theoretical study of pressure-driven phase transitions in HgSe and HgTe. *Phys. Rev. B*, 2011, 83, 094107.
[31] Duz I., Kart S.O., Erdem I., Kuzucu V. DFT study on phase transition behavior and mechanical properties of HgSe polymorphs under high pressure. *Current Applied Physics*, 2018, **18** (4), P. 424–436.
[32] Secuk M.N., Aycibin M., Erdinc B., Gulebaglan S.E., Dogan E.K., Akkus H. Ab-initio Calculations of Structural, Electronic, Optical, Dynamic and Thermodynamic Properties of HgTe and HgSe. *American J. of Condensed Matter Physics*, 2014, **4** (1), P. 13–19.
[33] Li J., He C., Meng L., Xiao H., Tang C., Wei X., Kim J., Kioussis N., Stocks G.M., Zhong J. Two-dimensional topological insulators with tunable band gaps: Single-layer HgTe and HgSe. *Scientific Reports*, 2015, **5** (1), 14115.
[34] Habibes N.E.H., Boukortt A., Meskine S., Benbedra A., Mamouni Y., Bennacer H. Electronic and Optical Properties of Mn-Doped HgSe Topological Insulator for Spintronic Devices. *ECS J. Solid State Sci. Technol.*, 2024, **13**, 013013.
[35] Ordejón P., Artacho E., Soler J.M. Self-consistent order N density functional calculations for very large systems. *Phys. Rev. B*, 1996, **53** (16), R10441–R10444.
[36] Soler J.M., Artacho E., Gale J.D., García A., Junquera J., Ordejón P., Portal D.S. The SIESTA method for ab initio order-N materials simulation. *J. Phys. Condens. Matter.*, 2002, **14** (11), P. 2745–2779.
[37] Perdew J.P., Burke K., Ernzerhof M. Generalized Gradient Approximation Made Simple. *Phys. Rev. Lett.*, 1997, **78**, 1396.
[38] Monkhorst H.J., Pack J.D. Special points for Brillouin-zone integrations. *Phys. Rev. B*, 1976, **13**, 5188.
[39] Zhao M., Xia Y., Zhang D., Mei L. Stability and electronic structure of AlN nanotubes. *Phys. Rev. B*, 2003, **68**, 235415.
[40] Das M., Mukherjee P., Chowdhury S., Gupta B.C. Tunable structural and electrical properties of zigzag CdS nanotubes: A density functional study. *Phys. Status Solidi B*, 2017, **254** (9), 1700038.
[41] Das M., Chowdhury S., Gupta B.C. Atomic-Ordering-Induced Modulated Properties of Zigzag ZnTe Nanotubes. *Phys. Status Solidi B*, 2021, **258** (8), 2100115.
[42] Senger R.T., Dag S., Ciraci S. Chiral Single-Wall Gold Nanotubes. *Phys. Rev. Lett.*, 2004, **93**, 196807.
[43] Pan H., Feng Y.P. Semiconductor Nanowires and Nanotubes: Effects of Size and Surface-to-Volume Ratio. *ACS Nano*, 2008, **2** (11), P. 2410–2414.
[44] Xiang H.J., Yang J., Hou J.G., Zhu Q. Piezoelectricity in ZnO nanowires: A first-principles study. *Appl. Phys. Lett.*, 2006, **89**, 223111.

Submitted 3 August 2024; revised 13 August 2024; accepted 14 August 2024

Information about the authors:

Monoj Das – Department of Physics, Gushkara Mahavidyalaya, Gushkara, 713128, India; ORCID 0000-0001-9367-2612; dsmonoj@gmail.com